Supporting information

The Effect of Potassium on the Steam-Methane Reforming on the Ni_4/Al_2O_3 Surface: A DFT study

Meng-Ru Li, Zhe Lu and Gui-Chang Wang*

(College of Chemistry, Key Laboratory of Advanced Energy Materials Chemistry (Ministry of Education) and Collaborative Innovation Center of Chemical Science and Engineering (Tianjin), Nankai University, Tianjin 300071, P. R. China)

*Corresponding author: Gui-Chang Wang. E-mail: wangguichang@nankai.edu.cn

Telephone: +86-22-23503824 (O) Fax: +86-22-23502458

S1 The physical origin of energy barrier in CH_3 and C formation

In order to get the insight of the main factor for the different barriers for CH_4 and CH species on Ni_4/Al_2O_3 and K pre-adsorbed Ni_4/Al_2O_3, the energetic method developed by Hammer[1] is used for reactions on clean and K pre-adsorbed Ni_4/Al_2O_3:$CH_4 \rightarrow CH_3+H$ and $CH \rightarrow C+H$. For reaction $AB \rightarrow A+B$, the barrier can be divided into five terms in equation (1):

$$Ea = \Delta E_{AB}^{g} + E_{AB}^{IS} + E_{\text{int}}^{TS} - E_{A}^{TS} - E_{B}^{TS} \quad (1)$$

Where ΔE_{AB}^{g}, E_{AB}^{IS}, E_{int}^{TS}, E_{A}^{TS} and E_{B}^{TS} refer to the bond energy of the gas-phase AB,

the adsorption energy of AB in the IS, a quantitative measurement of interaction between A and B in TS and the adsorption energy of A and B at the TS geometry, respectively.

$CH_4 \rightarrow CH_3+H$ On Ni_4/Al_2O_3 and K pre-adsorbed Ni_4/Al_2O_3, K will promote the C-H scission with a lower barrier of 0.54 eV than that on clean Ni_4/Al_2O_3 (0.63 eV). The interaction between CH_3 and H in TS (E_{int}^{TS}) on clean and K pre-adsorbed Ni_4/Al_2O_3 are approximate shown in Table S1. The higher adsorption energies of CH_3 (E_A^{TS}) and H species (E_B^{TS}) in TS on K pre-adsorbed Ni_4/Al_2O_3 will make up the higher adsorption energy of CH_4 in IS (E_{AB}^{IS}) on K pre-adsorbed Ni_4/Al_2O_3, which gives rise to the lower barrier at the presence of K. As a result, the stronger interaction between the TS species and catalyst (E_A^{TS} and E_B^{TS}) contributes to the promotion effect of K on C-H cleavage in CH_4.

In conclusion, the adsorption energy of TS species is the main factor for the promotion effect of K: the higher adsorption energy of TS species (CH_3 and H species) on K pre-adsorbed Ni_4/Al_2O_3 will decrease the barrier of C-H scission in CH_4. Since the adsorption energy of CH_4 in IS are weak and approximate, the adsorption energies of the CH_3 and H species in TS configuration will be related to the adsorption energies of the CH_3 and H species closely. As shown in Table 1, the higher adsorption energies of CH_3 and H species on K pre-adsorbed Ni_4/Al_2O_3 are in good agreement with the higher adsorption energies of the CH_3 and H species in TS configuration.

CH→C+H On clean and K pre-adsorbed Ni_4/Al_2O_3, the adsorption energies of CH species on clean and K pre-adsorbed Ni_4/Al_2O_3 are -6.64 eV and -6.56 eV. The adsorption energy of H species in TS configuration ($-E_B^{TS}$) on K pre-adsorbed

Ni_4/Al_2O_3 is -1.61 eV which is higher than that on clean Ni_4/Al_2O_3 (-0.95 eV). However, the lower adsorption energy of C species in TS configuration ($-E_A^{TS}$) which is equal to -6.76 eV and the weaker interaction term E_{int}^{TS} (-0.62 eV) give rises to the higher barrier on $Ni_4/K\text{-}Al_2O_3$. Among all the factors, we observed that the lower adsorption energy of the C species in TS configuration E_A^{TS} is the main factor for the higher barrier on K pre-adsorbed Ni_4/Al_2O_3, and the adsorption energy of the C species in TS configuration is supposed to be related to the lower adsorption energy of the C species on $Ni_4/K\text{-}Al_2O_3$ than that on clean Ni_4/Al_2O_3 (-7.56 eV versus -7.40 eV for clean and K pre-adsorbed Ni_4/Al_2O_3).

From the discussion above, it is obvious that the adsorption terms of TS are always the main factor affecting the barrier. Especially, the adsorption energies of CH_3 and C in TS geometry contribute to the different effects of K on C-H cleavage, and are supposed to be resulted from the adsorption energies of the CH_3 and H species. As shown in Figure S1(a), the K promotion effect on C-H cleavage increases in the first steps while the inhibition effect of K on C-H cleavage in the CH_2 and CH species turns stronger with the dehydrogenation steps going on. Furthermore, we will analysis the physical factor for K effect in the consecutive C-H cleavages forming CH_x below.

Table S1 Energy decomposition of the activation barrier in the dissociation of CH_x on clean and K pre-adsorbed Ni_4/Al_2O_3 (unit: eV)

Elementary step		ΔE_{AB}^{g}	E_{AB}^{IS}	E_{int}^{TS}	E_A^{TS}	E_B^{TS}
$CH_4 \rightarrow CH_3+H$	Ni_4/Al_2O_3	4.85	-0.05	0.04	1.98	2.23
	$Ni_4/K\text{-}Al_2O_3$	4.85	0.14	0.08	2.11	2.42

$CH_3 \rightarrow CH_2+H$	Ni_4/Al_2O_3	5.04	2.40	-0.44	4.11	2.09
	$Ni_4/K\text{-}Al_2O_3$	5.04	2.42	-0.08	4.48	2.37
$CH_2 \rightarrow CH+H$	Ni_4/Al_2O_3	4.84	4.28	-0.55	6.47	1.74
	$Ni_4/K\text{-}Al_2O_3$	4.84	4.63	-0.56	6.59	1.65
$CH \rightarrow C+H$	Ni_4/Al_2O_3	3.54	6.64	-1.10	7.41	0.95
	$Ni_4/K\text{-}Al_2O_3$	3.54	6.56	-0.62	6.76	1.61

Note: A and B refer to the CH_x and H species.

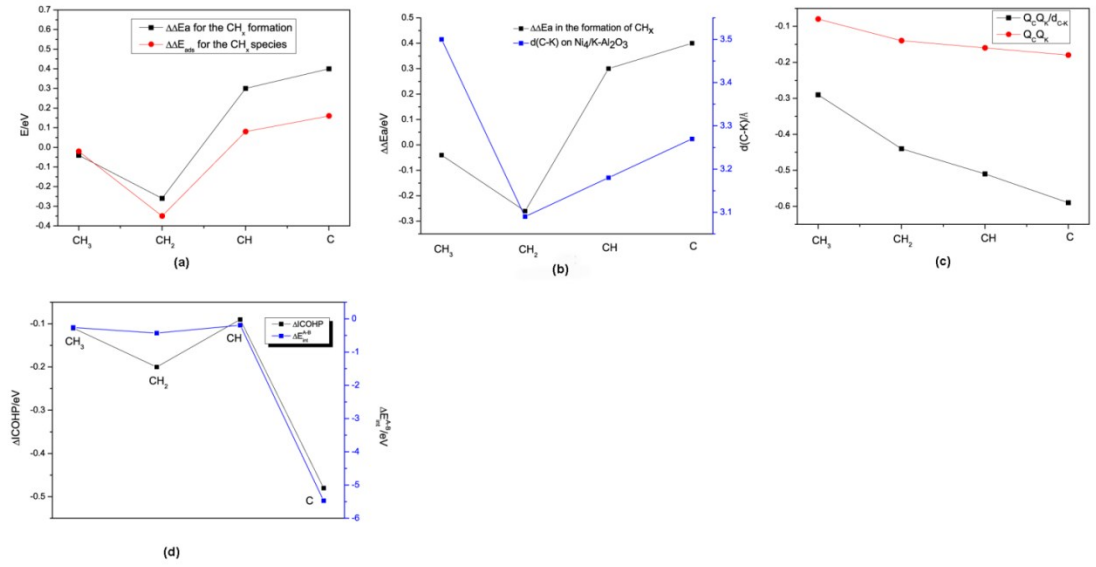

Figure S1. The change of ΔΔEa for the CH_x species formation and $\Delta\Delta E_{ads}$ for CH_x species with x ranging from 3 to 0 (a); The change of the distance between C and K in CH_x species (d(C-K)) with x ranging from 3 to 0 (b); The $Q_C Q_K$ and $\frac{Q_C Q_K}{d_{C-K}}$ with x ranging from 3 to 0 (c); The ΔICOHP for C-Ni interaction on K pre-adsorbed and clean Ni_4/Al_2O_3 and $\Delta E_{\text{int}}^{A-B}$ with x ranging from 3 to 0

Note: ΔΔEa refers to the difference between the barriers of the CH_x species formation on K pre-adsorbed and clean Ni_4/Al_2O_3, $\Delta\Delta E_{ads}$ is denoted as the difference between the adsorption energies of the CH_x species on K pre-adsorbed and clean Ni_4/Al_2O_3, ΔICOHP is the difference between the integrated COHP values of the interaction of C-Ni in CH_x species on K pre-adsorbed and clean Ni_4/Al_2O_3. $\Delta E_{\text{int}}^{A-B}$ is the difference of the interaction energy between the CH_x species and catalyst on K pre-adsorbed and clean Ni_4/Al_2O_3. Q_C and Q_K is calculated by Bader

charge analysis shown in Table S1 in the supporting information.

S2 The physical origin of Ea in CH_x formation

As is shown in Figure S1(a), the reaction barrier difference of C-H scission yielding CH_x (x=0-3) species between K pre-adsorbed and clean Ni_4/Al_2O_3 ($\Delta\Delta$Ea) various from -0.04 eV, -0.26 eV to 0.30 eV and 0.40 eV. The K effect turns from promotion effect to inhibition effect on the C-H scission forming CH_x. In order to explore the origin of the physical factor of the change, we divided the barrier along the dehydrogenation process. From Table S1, it could be obtained that generally the adsorption energy of CH_x species in TS configuration ($-E_A^{TS}$) is the main factor for the barrier. The adsorption energies of the CH_x species in TS configuration are related to the adsorption energies of the corresponding resulted species as the CH_3, CH_2, CH and C species. In addition, Figure S1(a) shows the adsorption energies difference of CH_x between K pre-adsorbed and clean Ni_4/Al_2O_3 ($\Delta\Delta E_{ads}$) will decrease from -0.02 eV in CH_3 species to -0.35 eV in CH_2 species firstly, and then increases to 0.08 and 0.16 eV in CH and C species, respectively. The trend of the adsorption energy of CH_x species is in line with that for the reaction barrier.

In conclusion, we find that the effect of K on the C-H scission forming CH_x changes from the promotion effect to inhibition effect with the dehydrogenation steps going on. Furthermore, the change is supposed to be resulted from the changing effect of K on the adsorption energy of CH_x. As a result, we will further explore the origin of changing effect of K on the CH_x species adsorption properties.

S3 The physical origin of E_{ads} of CH_x species

In order to get the insight of the K effect on the adsorption energy of CH_x species. We dissociate the adsorption energies of CH_x species on clean and K pre-adsorbed Ni_4/Al_2O_3 into the deforming energy items and the interaction energy items corresponding to the interaction between the adsorbate and the catalyst:

$$E_{ads} = (E_A - E_A^g) + (E_B - E_B^g) + E_{\text{int}}^{A-B} = E_A^{deform} + E_B^{deform} + E_{\text{int}}^{A-B} \quad (2)$$

where the first two items E_A^{deform} and E_B^{deform} refer to the deforming energies which are required to deform the geometries of the adsorbate in gas (E_A^g) and the catalyst (E_B^g) before the adsorption process to the geometries of the adsorbate (E_A) and the catalyst (E_B) after the adsorption process. The last item E_{int}^{A-B} corresponds to the binding energy between the deformed adsorbate and catalyst. The interaction item E_{int}^{A-B} is assumed to be dissociated into three components in equation (3)[2-4]:

$$E_{\text{int}}^{A-B} = E_{elstat} + E_{Pauli} + E_{orb} \quad (3)$$

where E_{elstat} is the electrostatic interaction energy between the fragments, E_{Pauli} represents the repulsion interaction between the fragments and is responsible for any steric repulsion, E_{orb} refers to the 2-electron stabilizing interaction between occupied levels of one fragment and empty levels of the other.

Table S2 Energy decomposition of the adsorption energy of CH_x on clean and K pre-adsorbed Ni_4/Al_2O_3 (unit: eV)

Species		E_A^{deform}	E_B^{deform}	E_{int}^{A-B}	ΔE_A^{deform}	ΔE_B^{deform}	$\Delta E_{\text{int}}^{A-B}$
CH_3	Ni_4/Al_2O_3	0.42	0.10	-2.92	0.16	0.08	-0.26

	$Ni_4/K\text{-}Al_2O_3$	0.58	0.18	-3.18			
CH_2	Ni_4/Al_2O_3	0.04	0.22	-4.28	0.06	0.02	-0.43
	$Ni_4/K\text{-}Al_2O_3$	0.10	0.24	-4.97			
CH	Ni_4/Al_2O_3	-0.01	0.58	-6.64	0.01	0.26	-0.19
	$Ni_4/K\text{-}Al_2O_3$	-0.00	0.84	-7.40			
C	Ni_4/Al_2O_3	0.13	1.34	-9.03	0.00	5.64	-5.47
	$Ni_4/K\text{-}Al_2O_3$	0.13	6.97	-14.51			

Note: E_A^{deform} (E_B^{deform}) refers to the deforming energy of CH_x (catalyst) which is the energy difference between the energies of the absorbed CH_x species (catalyst) geometry in CH_x-adsorbed catalyst and gas phase; E_{int}^{A-B} refer to the actual interaction energy between deformed CH_x and catalyst geometry; ΔE_A^{deform} (ΔE_B^{deform}) refer to the energy difference between the deforming energies of the absorbed CH_x species (catalyst) geometry E_A^{deform} (E_B^{deform}) on K pre-adsorbed and clean Ni_4/Al_2O_3, $\Delta E_{\text{int}}^{A-B}$ refer to the energy difference of the interaction energies between the absorbed CH_x species and catalyst geometry E_{int}^{A-B} on K pre-adsorbed and clean Ni_4/Al_2O_3.

From Table S2, on clean Ni_4/Al_2O_3, it is observed that the deforming energies of the CH_x species E_A^{deform} rang from 0.42 eV in CH_3, 0.04 eV in CH_2, -0.01 eV in CH to 0.13 eV in C. On the other hand, the deforming energies of the catalyst E_B^{deform} in the adsorption of CH_x species increases from 0.10 eV (CH_3), 0.22 eV (CH_2), 0.58 (CH) to 1.34 eV (C). In addition, the interaction energies for the interaction between the adsorbate CH_x species and catalyst E_{int}^{A-B} on clean Ni_4/Al_2O_3 increases form -2.92 eV (CH_3), -4.28 eV (CH_2), -6.64 eV(CH) to -9.03 (C). It is obvious that the difference of the deforming energies of CH_x species E_A^{deform} is little and could be ignored. The deforming energies of the catalyst E_B^{deform} keep increasing trend with the dehydrogenation of the CH_3 species into C. The interaction between the catalyst and

the CH_x E_{int}^{A-B} increases with the dehydrogenation of CH_3 into the C species.

On K pre-adsorbed Ni_4/Al_2O_3, the deforming energies of CH_x species E_A^{deform} is approximate to each other. The deforming energies of catalyst E_B^{deform} increases from 0.18 eV(CH_3), 0.24 eV(CH_2), 0.84 eV(CH) to 6.97 eV (C). On the other hand, the interaction energies for the interaction between CH_x species and catalyst E_{int}^{A-B} increases from -3.18 eV (CH_3), -4.97 eV (CH_2), -7.40 eV (CH) to -14.51 eV (C). The increasing interaction energies for the interaction between catalyst and CH_x species E_{int}^{A-B} could make up the increasing deforming energies of catalyst E_B^{deform}, which leads to the increasing adsorption energy of the CH_x species with the dehydrogenation steps going on.

In order to get the change of the deforming energy items and the interaction energy items with the addition of K, we compare the deforming energy items (E_A^{deform} and E_B^{deform}) and the interaction energy item (E_{int}^{A-B}) on clean and K pre-adsorbed Ni_4/Al_2O_3. From Table S2, we can observe that the difference of the deforming energies of the CH_x species on clean and K pre-adsorbed Ni_4/Al_2O_3 ΔE_A^{deform} is negligible and should be ignored. For CH_3 and CH_2 species adsorption, the interaction energy for the interaction between the catalyst and CH_x on $Ni_4/K\text{-}Al_2O_3$ is higher than that on clean Ni_4/Al_2O_3 reflected by the negative interaction energy difference for the interaction between the catalyst and CH_x on K pre-adsorbed and clean Ni_4/Al_2O_3 ΔE_{int}^{A-B}. Moreover, the more negative interaction energy difference ΔE_{int}^{A-B} along the dehydrogenation from CH_3 to CH_2 species contributes to the more negative adsorption energy difference of CH_x species on K pre-adsorbed and clean Ni_4/Al_2O_3. For CH and C species adsorption, the deforming energy of the catalyst E_B^{deform} on K pre-adsorbed

Ni_4/A_2O_3 is much higher than that on clean Ni_4/Al_2O_3 reflected by the positive deforming energy difference of catalyst on Ni_4/K-Al_2O_3 and clean Ni_4/Al_2O_3 ΔE_B^{deform}. The more positive deforming energy difference ΔE_B^{deform} along the dehydrogenation from CH to C species leads to the more positive adsorption energy difference of CH_x species on K pre-adsorbed and clean Ni_4/Al_2O_3.

In conclusion, the higher interaction between the catalyst and CH_x species on K pre-adsorbed Ni_4/Al_2O_3 E_{int}^{A-B} contributes to the promotion effect of K on the adsorption of CH_3 and CH_2 species. Furthermore, the increasing interaction difference between the catalyst and CH_x species on K pre-adsorbed and clean Ni_4/Al_2O_3 $\Delta E_{\text{int}}^{A-B}$ leads to the increasing promotion effect of K on the adsorption energies of CH_3 and CH_2. For the adsorption of CH and C, the higher deforming energy of Ni_4/K-Al_2O_3 E_B^{deform} leads to the inhibition effect of K on the adsorption of CH and C species. And the increasing deforming energy difference of catalyst on K pre-adsorbed and clean Ni_4/Al_2O_3 ΔE_B^{deform} contributes to the increasing inhibition effect of K on the adsorption energies of CH and C species. Hence we will explore the insight of the increasing interaction energy difference between the CH_x species and the catalyst $\Delta E_{\text{int}}^{A-B}$ and the increasing deforming energy difference of the catalyst ΔE_B^{deform} in the next part.

S4 The physical origin of $\Delta E_{\text{int}}^{A-B}$ of CH_x species

In order to get the insight of the interaction energies between the CH_x species and the catalyst E_{int}^{A-B}, we will divide the interaction energies into three parts: E_{elstat}, E_{Pauli} and E_{orb} in equation (3). As the interaction energies between the CH_x species and the

catalyst E_{int}^{A-B} are negative (Table S2), the interaction between the CH_x species and the catalyst is attractive interaction rather than repulsion interaction. As a result, the interaction between CH_x species and the catalyst is mainly determined by E_{elstat} and E_{orb}. For the electrostatic interaction energy between the catalyst and CH_x (E_{elstat}), as the CH_x species is mainly adsorbed through C with Ni and K, we mainly measure the electrostatic interaction between C and Ni (K). For the electrostatic interaction energy is proportional to $\frac{Q_C Q_{Ni(K)}}{d_{C-Ni(K)}}$, we measure the electrostatic interaction energy between the C and Ni (K) through $\frac{Q_C Q_{Ni(K)}}{d_{C-Ni(K)}}$ shown in Figure S1(c). Compared with the electrostatic interaction between C and K, the electrostatic interaction between C and Ni is rather lower and should be ignored. The electrostatic interaction item $\frac{Q_C Q_K}{d_{C-K}}$ between C and K increases from -0.08 (CH_3), -0.14 (CH_2), -0.16 (CH) to -0.18 (C). The negative value between K and Ni indicates the attractive interaction between K and Ni. The electrostatic interaction between C and K keeps increasing trend along the dehydrogenation. However, the $\Delta E_{\text{int}}^{A-B}$ will turn to decrease from CH_2 to CH species. The increasing electrostatic interaction E_{elstat} between C and K could hardly fit the changing trend of $\Delta E_{\text{int}}^{A-B}$.

For the orbital overlapping energy E_{orb}, we use the crystal orbital Hamilton populations (COHPs)[5-8] to investigate the insight of the K effect on the orbital overlapping energy E_{orb} of CH_x species. The COHP curves of C-K, Ni-K and C-Ni interaction on K pre-adsorbed Ni_4/Al_2O_3 are shown in Figure S2. The Integrated COHP (ICOHP) value could reflect the orbital interaction between two atoms. The

negative value corresponds to the stronger interaction between orbitals. The integrated COHP values for C-K, Ni-K and C-Ni interaction are established in Table S3.

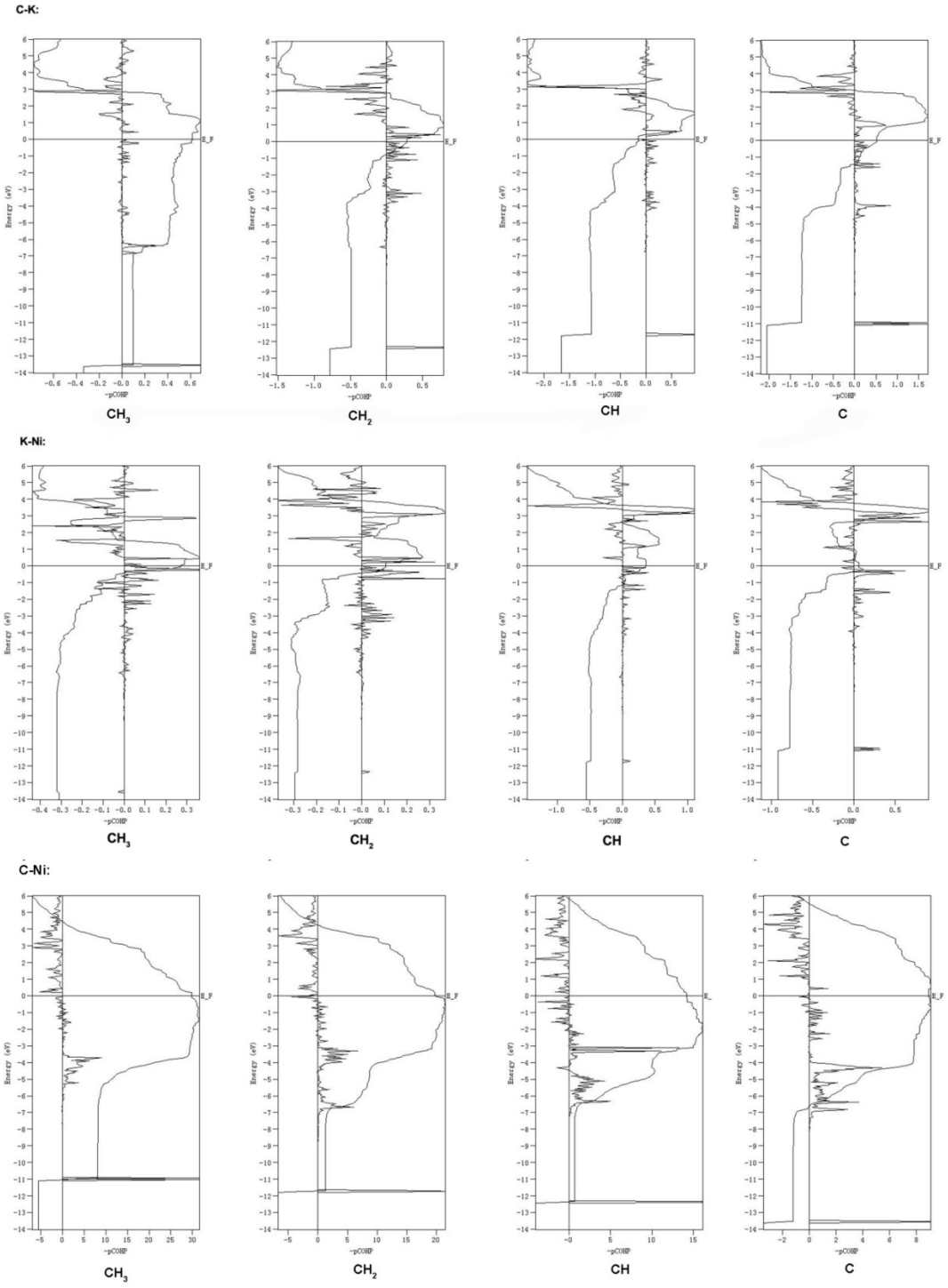

Figure S2. The COHP curves for the interaction between K and C, the interaction between K and Ni, and the interaction between C and Ni in CH_3, CH_2, CH and C species on $Ni_4/K\text{-}Al_2O_3$;

Table S3 Integrated COHPs (eV)

Species		C-K	K-Ni	C-Ni	$\Delta E_{\text{int}}^{A-B}$	ΔICOHP
CH_3	Ni_4/Al_2O_3	-	-	-1.22	-0.26	-0.11
	$Ni_4/K\text{-}Al_2O_3$	-0.03	-0.04	-1.34		
CH_2	Ni_4/Al_2O_3	-	-	-1.56	-0.43	-0.20
	$Ni_4/K\text{-}Al_2O_3$	-0.09	-0.04	-1.75		
CH	Ni_4/Al_2O_3	-	-	-1.92	-0.19	-0.09
	$Ni_4/K\text{-}Al_2O_3$	-0.05	-0.08	-2.01		
C	Ni_4/Al_2O_3	-	-	-1.82	-5.47	-0.48
	$Ni_4/K\text{-}Al_2O_3$	-0.14	-0.08	-2.30		

Note: $\Delta E_{\text{int}}^{A-B}$ refer to the energy difference of the interaction energies between the absorbed CH_x species and catalyst geometry on K pre-adsorbed and clean Ni_4/Al_2O_3. The ΔICOHP is the difference of the ICOHP value for the interaction between C and Ni neighboring K on K pre-adsorbed and clean Ni_4/Al_2O_3.

On K pre-adsorbed Ni_4/Al_2O_3, we find that the ICOHP values of the interaction between C and K are much lower than that for the interaction between C and Ni shown in Table S3. Hence, we will focus on the ICOHP values of the interaction between C and Ni. Furthermore, the ICOHP value of the interaction between C and Ni neighboring K is higher than that for the interaction between C and other Ni atoms. The ICOHP value for the interaction between C and Ni neighboring K majors the orbital interaction between CH_x and the catalyst. We use the difference of the ICOHP values for the interaction between C and Ni neighboring K on K pre-adsorbed and that

for the corresponding C and Ni interaction on clean Ni_4/Al_2O_3 (ΔICOHP in Table S3) to measure the K effect on the orbital overlapping energies E_{orb}. The values of ΔICOHP change from -0.11 eV (CH_3), -0.20 eV (CH_2), -0.09 eV (CH) to -0.48 eV (C), the trend of which agrees well with that for the $\Delta E_{\text{int}}^{A-B}$ shown in Figure S1d.

Based on the above discussion, it is concluded that K will promote the interaction between CH_x species and catalyst through the E_{elstat} and E_{orb}: the increasing attractive electrostatic interaction between C and K and the increasing overlapping orbitals of C and Ni neighboring K. Furthermore, K will influence the interaction between CH_x and catalyst mainly through enhancing the overlapping of the orbitals of C and Ni, which is different from the electrostatic interaction lying in the K inhibition effect in the previous study[9]. It could be explained: for the increasing electrostatic interaction between C and K (E_{elstat}), K could donate electron to Ni neighboring K, and K will carry positive charge. From Table S4, it is observed that the positive charge of K almost remains +0.85 with the hydrogenation going on. On the other hand, with the hydrogenation steps going on, the C will bind to more Ni atoms and Ni will donate more electrons to C reflected by the more negative charge of C shown in Table S4. Therefore the attractive electrostatic interaction between C and K increases. For the increasing overlapping orbitals of C and Ni neighboring K (E_{orb}), K could enhance the overlapping the orbitals of the Ni and C through donating more electron to Ni.

Table S4. The charge of atoms (C, K and Ni) on CH_x-adsorbed $Ni_4/K\text{-}Al_2O_3$

calculated by Bader Charge Analysis

Species	C	K	Ni	Ni	Ni
CH_3	-0.34	+0.85	+0.04	+0.01	-
CH_2	-0.52	+0.84	-0.07	-0.01	-
CH	-0.62	+0.82	-0.09	+0.02	+0.07
C	-0.69	+0.85	+0.08	-0.04	+0.00

Note: Only the charge of Ni atoms which are binding to CH_x species is calculated.

Table S5 Energy decomposition of $E^{deform}_{catalyst(Ni_4/\mathrm{K}-Al_2O_3)}$ on K pre-adsorbed Ni_4/Al_2O_3 (unit: eV)

Species	$E^{deform}_{catalyst(Ni_4/Al_2O_3)}$	$E^{deform}_{catalyst(Ni_4/\mathrm{K}-Al_2O_3)}$	ΔE^{deform}_{K}	$\Delta E^{deform}_{Ni_4/Al_2O_3}$	$\Delta E^{K-Ni_4/Al_2O_3}_{\mathrm{int}}$
CH_3	0.10	0.18	0.00	0.19	0.00
CH_2	0.22	0.24	-0.04	0.13	0.15
CH	0.57	0.84	0.00	0.91	-0.07
C	1.34	6.97	0.00	0.78	6.20

Note: $E^{deform}_{catalyst(Ni_4/\mathrm{K}-Al_2O_3)}$ ($E^{deform}_{catalyst(Ni_4/Al_2O_3)}$) refers to the deforming energy of catalyst Ni_4/K-Al_2O_3 (Ni_4/Al_2O_3); ΔE^{deform}_{K} and $\Delta E^{deform}_{Ni_4/Al_2O_3}$ refer to the deforming energy of K atom and the Ni_4/Al_2O_3 geometry; $\Delta E^{K-Ni_4/Al_2O_3}_{\mathrm{int}}$ refer to the energy difference of the interaction energies between K and Ni_4/Al_2O_3 on the CH_x-absorbed and clean Ni_4/K-Al_2O_3.

(d) The physical origin of ΔE^{deform}_{B} For the inhibition effect of K on the adsorption energy of CH and C, we find that it is the high deforming energies of catalyst causing the lower adsorption energies of CH and C species at the presence of K. In order to get the insight of the higher deforming energies of K pre-adsorbed Ni_4/Al_2O_3, we divided the deforming energy into the deforming energies of K and Ni_4/Al_2O_3 and the changing interaction energy for the interaction between K and Ni_4/Al_2O_3 in equation (4):

$$\Delta E^{deform}_{catalyst} = (E^{CHx}_{K} - E^{clean}_{K}) + (E^{CHx}_{Ni_4/Al_2O_3} - E^{clean}_{Ni_4/Al_2O_3}) + \Delta E^{K-Ni_4/Al_2O_3}_{\mathrm{int}} = \Delta E^{deform}_{K} + \Delta E^{deform}_{Ni_4/Al_2O_3} + \Delta E^{K-Ni_4/Al_2O_3}_{\mathrm{int}} \qquad (4)$$

Where E^{CHx}_{K} and $E^{CHx}_{Ni_4/Al_2O_3}$ refer to the energies of the K geometry and Ni_4/Al_2O_3 geometry on CH_x-adsorbed Ni_4/K-Al_2O_3. E^{clean}_{K} and $E^{clean}_{Ni_4/Al_2O_3}$ are denoted as the energies of the K geometry and Ni_4/Al_2O_3 geometry on clean Ni_4/K-Al_2O_3. $\Delta E^{K-Ni_4/Al_2O_3}_{\mathrm{int}}$ refers to the difference of the interaction energy for the interaction between K and Ni_4/Al_2O_3 on CH_x-adsorbed and clean Ni_4/K-Al_2O_3. The first two items ΔE^{deform}_{K} and $\Delta E^{deform}_{Ni_4/Al_2O_3}$ refer to the deforming energies of the K and Ni_4/Al_2O_3 geometry on CH_x-adsorbed Ni_4/K-Al_2O_3. The last item $\Delta E^{K-Ni_4/Al_2O_3}_{\mathrm{int}}$ represents the changing interaction between Ni_4/Al_2O_3 and K.

As shown in Table S5, the deforming energies of K ΔE_K^{deform} on CH_x-adsorbed Ni_4/K-Al_2O_3 are negligible. However, the deforming energies of Ni_4/Al_2O_3 $\Delta E_{Ni_4/Al_2O_3}^{deform}$ turn to increase significantly in CH-adsorbed Ni_4/K-Al_2O_3. It is the higher deforming energies of Ni_4/Al_2O_3 geometry $\Delta E_{Ni_4/Al_2O_3}^{deform}$ leading to the lower adsorption energy of the CH species. The large deform of Ni_4/Al_2O_3 is caused by the steric hindrance lying in CH, Ni and K. For the C species, the difference of the interaction energy between K and Ni_4/Al_2O_3 $\Delta E_{\text{int}}^{K-Ni_4/Al_2O_3}$ is much higher on C-adsorbed Ni_4/K-Al_2O_3 and is responsible for the inhibition effect of K on C adsorption. For K will interact with Ni_4/Al_2O_3 through the interaction between K and Ni, we will explore the interaction between K and Ni from three aspects: E_{elstat}, E_{Pauli} and E_{orb}. For the electrostatic interaction energy E_{elstat} between K and Ni_4/Al_2O_3, it is found that the electrostatic interaction energy between K and Ni is negative and is not responsible for the repulsion interaction between K and Ni. For the overlapping energy E_{orb}, the ICOHP value for the interaction between Ni and K is -0.08 eV on C-adsorbed Ni_4/Al_2O_3, which indicates that the overlapping energy E_{orb} fails to explain the repulsion interaction between K and Ni_4/Al_2O_3. Hence the repulsion interaction between the K and Ni_4/Al_2O_3 is responsible for the repulsion interaction between K and Ni_4/Al_2O_3.

In conclusion, with the dehydrogenation steps going on, the CH and C species will bind to more Ni atoms, which could compete with the interaction between Ni and K yielding the steric repulsion. It is observed that the steric repulsion in CH(C)-adsorbed Ni_4/K-Al_2O_3 will increase significantly and lead to the deformation of the Ni_4/K-

Al_2O_3 reflected by larger values of $\Delta E^{deform}_{Ni_4/Al_2O_3}$ on CH(C)-adsorbed Ni_4/K-Al_2O_3 shown in Table S5. The deformation of the Ni_4/K-Al_2O_3 mainly includes the deformation of Ni_4/Al_2O_3 $\Delta E^{deform}_{Ni_4/Al_2O_3}$ and the displacement of K reflected by the interaction between Ni and K $\Delta E^{K-Ni_4/Al_2O_3}_{\text{int}}$. On CH-adsorbed Ni_4/K-Al_2O_3, the K will bind to Ni stably, which leads to the deforming of Ni_4 to release the repulsion interaction yielding high deforming energy of Ni_4/Al_2O_3 ($\Delta E^{deform}_{Ni_4/Al_2O_3}$). On C-adsorbed Ni_4/K-Al_2O_3, the interaction between C and Ni grows stronger with the hydrogenation going on and turns stronger than that for K and Ni_4/Al_2O_3, which will stabilize the Ni_4/Al_2O_3. The deforming of Ni_4 decreases on C-adsorbed Ni_4/K-Al_2O_3 compared with that on CH-adsorbed Ni_4/K-Al_2O_3 reflected by the less deforming energy of Ni_4/Al_2O_3 $\Delta E^{deform}_{Ni_4/Al_2O_3}$ (0.78 eV versus 0.91 eV for $\Delta E^{deform}_{Ni_4/Al_2O_3}$ on C and CH-adsorbed Ni_4/Al_2O_3, respectively). Instead, the repulsion interaction will be released by the displacement of K reflected by the longer distance of K-Ni on C-adsorbed Ni_4/K-Al_2O_3 than that on CH-adsorbed Ni_4/K-Al_2O_3 (3.14 Å and 3.36 Å for d(Ni-K) on CH and C-adsorbed Ni_4/K-Al_2O_3, respectively) which corresponds to the larger repulsion interaction between K and Ni_4 $\Delta E^{K-Ni_4/Al_2O_3}_{\text{int}}$.

Table S6 the charge of Ni on Ni_4 on clean and K pre-adsorbed Ni_4/Al_2O_3 shown in Figure 7

catalyst	Ni41	Ni42	Ni43	Ni44
Ni_4/Al_2O_3	-0.10	-0.05	-0.10	-0.19

Ni_4/KAl_2O_3	-0.24	-0.25	-0.22	-0.46

References and Notes

1. B. Hammer, *Surface Science*, 2000, **459**, 323-348.
2. F. M. Bickelhaupt and E. J. Baerends, *Reviews in Computational Chemistry*, 2000, **15**, 1-86.
3. A. Kovács, C. Esterhuysen and G. Frenking, *Chemistry*, 2005, **11**, 1813-1825.
4. J. Poater, M. Sola and F. M. Bickelhaupt, *Chemistry*, 2006, **12**, 2889-2895.
5. V. L. Deringer, A. L. Tchougreeff and R. Dronskowski, *The Journal of Physical Chemistry. A*, 2011, **115**, 5461-5466.
6. S. Maintz, V. L. Deringer, A. L. Tchougreeff and R. Dronskowski, *J Comput Chem*, 2016, **37**, 1030-1035.
7. R. Dronskowski and P. E. Bloechl, *J.phys.chem*, 1993, **97**, 8617-8624.
8. S. Maintz, V. L. Deringer, A. L. Tchougréeff and R. Dronskowski, *Journal of Computational Chemistry*, 2013, **34**, 2557-2567.
9. H. S. Bengaard, I. Alstrup, I. Chorkendorff, S. Ullmann, J. R. Rostrup-Nielsen and J. K. Nørskov, *Journal of Catalysis*, 1999, **187**, 238-244